0026-895X/07/7101-284–293$20.00
MOLECULAR PHARMACOLOGY
Copyright © 2007 The American Society for Pharmacology and Experimental Therapeutics
Mol Pharmacol 71:284–293, 2007

Vol. 71, No. 1
28530/3165072
Printed in U.S.A.

Neurokinin 1 Receptors Trigger Overlapping Stimulation and Inhibition of $Ca_V2.3$ (R-Type) Calcium Channels

Ulises Meza, Ashish Thapliyal, Roger A. Bannister, and Brett A. Adams

Department of Physiology and Pharmacology, Universidad Autónoma de San Luis Potosí, San Luis Potosí, México (U.M.); and Department of Biology, Utah State University, Logan, Utah (A.T., R.A.B., B.A.A.)

Received July 5, 2006; accepted October 18, 2006

ABSTRACT

Neurokinin (NK) 1 receptors and $Ca_V2.3$ calcium channels are both expressed in nociceptive neurons, and mice lacking either protein display altered responses to noxious stimuli. Here, we examined modulation of $Ca_V2.3$ through NK1 receptors expressed in human embryonic kidney 293 cells. We find that NK1 receptors generate complex modulation of $Ca_V2.3$. In particular, weak activation of these receptors evokes mainly stimulation of $Ca_V2.3$, whereas strong receptor activation elicits profound inhibition that overlaps with channel stimulation. Unlike R-type channels encoded by $Ca_V2.3$, L-type ($Ca_V1.3$), N-type ($Ca_V2.2$), and P/Q-type ($Ca_V2.1$) channels are inhibited, but not stimulated, through NK1 receptors. Pharmacological experiments show that protein kinase C (PKC) mediates stimulation of $Ca_V2.3$ through NK1 receptors. The signaling mechanisms underlying inhibition were explored by expressing proteins that buffer either $G\alpha_{q/11}$ (regulator of G protein signaling protein 3T and carboxyl-terminal region of phospholipase C-β1) or $G\beta\gamma$ subunits (transducin and the carboxyl-terminal region of bovine G-protein-coupled receptor kinase). A fast component of inhibition was attenuated by buffering $G\beta\gamma$, whereas a slow component of inhibition was reduced by buffering $G\alpha_{q/11}$. When both $G\beta\gamma$ and $G\alpha_{q/11}$ were simultaneously buffered in the same cells, inhibition was virtually eliminated, but receptor activation still triggered substantial stimulation of $Ca_V2.3$. We also report that NK1 receptors accelerate the inactivation kinetics of $Ca_V2.3$ currents. Altogether, our results indicate that NK1 receptors modulate $Ca_V2.3$ using three different signaling mechanisms: a fast inhibition mediated by $G\beta\gamma$, a slow inhibition mediated by $G\alpha_{q/11}$, and a slow stimulation mediated by PKC. This new information concerning R-type calcium channels and NK1 receptors may help in understanding nociception, synaptic plasticity, and other physiological processes.

R-type Ca^{2+} currents have been pharmacologically defined by their resistance to blockers of L-type, N-type, and P/Q-type Ca^{2+} channels (Zhang et al., 1993) and by their sensitivity to SNX-482, a peptide component of spider venom (Newcomb et al., 1998). Considerable evidence indicates that native R-type currents are mediated by $Ca_V2.3$ subunits (Piedras-Rentería and Tsien, 1998; Tottene et al., 2000; Lee et al., 2002; Sochivko et al., 2002). Recent studies have begun to elucidate the physiological roles of both R-type currents and $Ca_V2.3$. For example, R-type currents have been shown to participate in neurosecretion and in the formation of afterdepolarizations, plateau potentials, and bursting activity in hippocampal CA1 pyramidal neurons (Wu et al., 1998; Gasparini et al., 2001; Kuzmiski et al., 2005; Metz et al., 2005; Tai et al., 2006). Studies also indicate that native R-type channels mediate Ca^{2+} entry into dendritic spines (Sabatini and Svoboda, 2000) and that R-type channels play important roles in synaptic plasticity (Yasuda et al., 2003; Humeau et al., 2005). Likewise, $Ca_V2.3$ has been demonstrated to be involved in cerebellar function, morphine tolerance, and synaptic plasticity (Kubota et al., 2001; Breustedt et al., 2003; Dietrich et al., 2003; Yokoyama et al., 2004; Osanai et al., 2006). It is noteworthy that $Ca_V2.3$ is also implicated in nociception, as evidenced by the fact that $Ca_V2.3$ knockout mice exhibit functional deficits in pain perception (Saegusa et al., 2000) and intrathecal injection of SNX-482 produces analgesia (Murakami et al., 2004).

This work was supported by Consejo Nacional de Ciencia y Tecnologia grant 39865-Q and UASLP grant C06-FAI-03-4.7 (to U.M.) and by Muscular Dystrophy Association grant MDA3663 and the Utah Agricultural Experimental Station Project UTA00581 (to B.A.A.).

Portions of this work were previously presented at the 2003 and 2006 annual meetings of the Biophysical Society (*Biophys J Suppl* **84:**537a; *Biophys J Suppl* **90:**396a).

U.M. and A.T. contributed equally to this work.

Article, publication date, and citation information can be found at http://molpharm.aspetjournals.org.

doi:10.1124/mol.106.028530.

ABBREVIATIONS: NK, neurokinin; HEK, human embryonic kidney; PKC, protein kinase C; EGFP, enhanced green fluorescent protein; MAS-GRK3ct, carboxyl-terminal region of G protein-coupled receptor kinase 3; $G\alpha_t$, rod transducin; RGS3T, regulator of G protein signaling protein 3T; RGS2, regulator of G protein signaling protein 2; PLCβ1ct, carboxyl-terminal region (T^{903}-L^{1216}) of phospholipase C-β1; *C*, cell capacitance; R_S, series access resistance; NKA, neurokinin A; PTX, pertussis toxin; CTX, cholera toxin; Bis, bisindolylmaleimide; I-V, current-voltage; PP2, 4-amino-5-(4-chlorophenyl)-7-(*t*-butyl)pyrazolo[3,4-*d*]pyrimidine.

Several previous studies demonstrated that $Ca_V2.3$ and native R-type currents are modulated by signaling mechanisms linked to G protein-coupled receptors (Wu et al., 1998; Yu and Shinnick-Gallagher, 1998; Meza et al., 1999; Melliti et al., 2000; Sabatini and Svoboda, 2000; Bannister et al., 2004; Kohlmeier and Leonard, 2006; Tai et al., 2006). In our previous experiments, we showed that $Ca_V2.3$ is both inhibited and stimulated through $G\alpha_{q/11}$-coupled muscarinic acetylcholine receptors (Meza et al., 1999; Melliti et al., 2000; Bannister et al., 2004). The neurokinin (NK) 1 receptor is a $G\alpha_{q/11}$-coupled receptor with a well established role in nociception (Macdonald et al., 1996; Duffy, 2004). Responses to noxious stimuli are dramatically altered in NK1 receptor-knockout mice (De Felipe et al., 1998). NK1 receptors are expressed with $Ca_V2.3$ in primary sensory neurons, in projection neurons within the dorsal horn of the spinal cord, and in various regions of mammalian brain, including amygdala, hippocampus, and striatum (Niidome et al., 1992; Saegusa et al., 2000; Lee et al., 2002; Duffy, 2004; Murakami et al., 2004). Thus, NK1 receptors may modulate $Ca_V2.3$ in vivo, and such modulation may be important in anxiety, nociception, synaptic plasticity, and other neurological processes.

In the present study, we analyzed modulation of $Ca_V2.3$ by NK1 receptors expressed in human embryonic kidney (HEK) 293 cells. We show that NK1 receptors produce a robust and complex modulation of $Ca_V2.3$ that involves three distinct signaling mechanisms: a fast inhibition mediated by $G\beta\gamma$, a slow inhibition mediated by $G\alpha_{q/11}$, and a slow stimulation mediated by protein kinase C (PKC). To our knowledge, this is the first demonstration that $Ca_V2.3$ is inhibited through a $G\alpha_{q/11}$-dependent signaling mechanism. Our results indicate that NK1 receptors predominantly stimulate $Ca_V2.3$ in the presence of low agonist concentrations. By contrast, these receptors trigger profound inhibition that overlaps with stimulation of $Ca_V2.3$ in the presence of high agonist concentrations. Our findings provide new information about modulation of $Ca_V2.3$ that may be relevant to understanding pain transduction, neuronal excitability, and synaptic plasticity.

Materials and Methods

Cell Culture and Transfection. HEK293 cells (American Type Culture Collection, Manassas, VA) were propagated in culture medium containing 90% Dulbecco's modified Eagle's medium (Invitrogen, Carlsbad, CA), 10% defined fetal bovine serum (Hyclone Laboratories, Logan, UT) and 50 μg/ml gentamicin. Cells of low passage number (<20) were trypsinized weekly and replated onto 60-mm culture dishes at ~20% confluence. Cells were transfected by $CaPO_4$ precipitation within 3 to 5 days of plating. The transfection mixture contained a mixture of expression plasmids encoding $Ca_V2.3$ (or in selected experiments $Ca_V1.3$, $Ca_V2.1$, or $Ca_V2.2$) and ancillary Ca^{2+} channel $\alpha_2\delta$ and β_3 subunits (each at 1.25 μg/dish), the human NK1 receptor (0.29 μg/dish), and enhanced green fluorescent protein (EGFP; 0.125 μg/dish). The plasmid encoding unfused EGFP was omitted when peptides fused in-frame to EGFP were expressed (see below). In experiments with $Ca_V2.1$, the β_{1a} subunit was cotransfected in place of β_3 to enhance expression of P/Q-type current. In selected experiments, the transfection mixture included plasmids encoding human rod transducin ($G\alpha_t$) or the carboxyl-terminal region of bovine G protein-coupled receptor kinase 3 (GRK3ct) fused to a membrane-associating myristic acid attachment sequence (MAS-GRK3ct). We also expressed the following proteins fused in-frame to the carboxyl terminus of EGFP: human regulator of G protein signaling protein 3T (RGS3T), the carboxyl-terminal region (T^{903}-L^{1216}) of rat phospholipase C-β1 (PLCβ1ct), and the RGS domain (Q^{45}-Q^{170}) of human p115 RhoGEF (p115RGS), each at 1.25 μg/dish. The day after transfection, cells were briefly trypsinized, replated onto 12-mm round glass coverslips, and incubated at 37°C. Electrophysiological recordings were made 24 to 32 h later. Successfully transfected cells were visually identified under UV illumination. Only isolated green cells were used for experiments.

Expression Plasmids. Rabbit brain $Ca_V2.3$ (GenBank accession number X67856) was in pcDNA3.1$^+$ (Invitrogen). Rat brain $\alpha_2\delta$ (GenBank accession number M86621) was in pMT2 (Genetics Institute, Cambridge, MA). Rabbit brain β_3 (GenBank accession number X64300) was in pcDNA3 (Invitrogen). Rabbit skeletal muscle β_{1a} (GenBank accession number M25817) was in pKCRH2. Human NK1 receptor (GenBank accession number NM015727) was in pCI (Promega, Madison, WI). Jellyfish EGFP (GenBank accession number U55763) was in pEGFP-C3 (Clontech, Cambridge, UK). Human $G\alpha_t$ (GenBank accession number X63749) was in pcDNA3.1$^+$. Human RGS3T (GenBank accession number U27655) was in pEGFP-C3. Rat PLCβ1ct (GenBank accession number M20636) was in pEGFP-C1. Bovine MAS-GRK3ct (GenBank accession number NM_174500) was in pcDNA3.1$^+$. Human p115RGS (GenBank accession number U64105) was in pEGFP-C3 and pcDNA3.1$^-$.

Patch-Clamp Recordings. Large-bore patch pipettes were pulled from 100-μl borosilicate glass micropipettes and filled with internal solution containing 155 mM CsCl, 10 mM Cs_2-EGTA, 4 mM Mg-ATP, 0.32 mM Li-GTP, and 10 mM HEPES, with pH adjusted to 7.4 using CsOH. In one experiment, Li-GTP was replaced by 1 mM Li-GDPβS. Aliquots of pipette solutions were stored at −80°C, kept on ice after thawing, and filtered at 0.22 μm immediately before use. The bath solution contained 145 mM NaCl, 40 or (where indicated) 5 mM $CaCl_2$, 2 mM KCl, and 10 mM HEPES, with pH adjusted to 7.4 using NaOH. When filled with internal solution, pipettes had resistances of 1.0 to 1.5 MΩ. After forming a GΩ seal in the cell-attached configuration, residual pipette capacitance was compensated using the negative capacitance circuit of the amplifier. Ca^{2+} currents were recorded in whole-cell, ruptured-patch mode. The resistance of the whole-cell configuration was routinely >1 GΩ. The steady holding potential was −90 mV. No corrections were made for liquid junction potentials. Currents were filtered at 2 to 10 kHz using the built-in Bessel filter (four-pole low-pass) of an Axopatch 200B amplifier (Molecular Devices, Sunnyvale, CA) and sampled at 10 to 50 kHz using a Digidata 1200 or 1320A analog-to-digital board installed in a Gateway Pentium computer. The pCLAMP software programs Clampex and Clampfit (version 8.0; Molecular Devices) were used for data acquisition and analysis, respectively. Figures were made, and statistical analyses were performed using Origin (version 6.0 or 7.5; OriginLab Corp., Northampton, MA). Linear cell capacitance (C) was determined by integrating the area under the whole-cell capacity transient, evoked by a voltage-clamp step from −90 to −80 mV. Voltage errors (typically <5 mV) were minimized using the analog series-resistance compensation circuit of the amplifier to reduce the time constant for decay of the whole-cell capacity transient as much as possible. Voltage error was calculated as the product of maximal inward Ca^{2+} current and series access resistance (R_S). R_S was calculated as the time constant for the whole-cell capacity transient × (1/C). All currents were corrected on-line for linear capacitance and leakage currents using −P/4 subtraction. Ca^{2+} current amplitudes were measured at the time of peak inward current. All experiments were conducted at room temperatures (20–24°C). Results are reported as mean ± S.E.M. Data were analyzed using unpaired or paired t tests. The significance level was set at 0.05.

In all experiments, the recording chamber (RC-12; Warner Instruments, Hamden, CT) was continuously perfused at the rate of ~2 to 3 ml/min. Agonist application and washout were achieved by bulk exchange of the bath solution, and they were 90% complete within ~11 and ~27 s, respectively, as judged by block and unblock of $Ca_V2.3$ current by 0.1 mM Cd^{2+}. Temperature was continuously monitored using a small thermocouple placed in the bath.

Reagents. Neurokinin A (NKA), substance P, pertussis toxin (PTX), cholera toxin (CTX), staurosporine, bisindolylmaleimide (Bis) I, and Bis V were purchased from EMD Biosciences (San Diego, CA). NKA and substance P were dissolved in 5% acetic acid to make 1 mM stock solutions, aliquoted, and stored at −80°C. Staurosporine, Bis I, Bis V, and PP2 were dissolved in dimethyl sulfoxide to make 1 mM stock solutions, aliquoted, and stored at 4°C. The final concentrations of acetic acid and dimethyl sulfoxide were always <0.005 and <0.2%, respectively, which did not significantly alter basal properties of $Ca_V2.3$ or its modulation through NK1 receptors.

Results

Strongly Activated NK1 Receptors Inhibited the Amplitude, Altered the Voltage Dependence of Activation, and Accelerated Inactivation of $Ca_V2.3$ Currents. Figure 1A shows families of whole-cell Ca^{2+} currents recorded from an HEK293 cell that expressed both NK1 receptors and $Ca_V2.3$ channels. Currents were recorded from the same cell before and during application of 1 μM NKA. This concentration of NKA caused profound inhibition of $Ca_V2.3$ current amplitudes. On average, currents evoked at a test potential of +20 mV were inhibited by 57 ± 3% (n = 30). Figure 1B plots the averaged, normalized current-voltage (I-V) relationships for control and inhibited currents. Similar magnitudes of inhibition were observed at different test potentials (Fig. 1B), suggesting that NK1 receptors trigger a mostly voltage-independent inhibition of $Ca_V2.3$. In support of this idea, inhibited currents failed to exhibit prepulse facilitation (data not shown). However, as illustrated in Fig. 1B, the scaled I-V relationship for inhibited currents was shifted to negative potentials relative to control currents. This voltage shift was statistically significant ($p < 0.05$) over a narrow range of test potentials (−10 to 0 mV). These results show that strongly activated NK1 receptors inhibit $Ca_V2.3$ current amplitudes and shift the voltage dependence of activation to slightly more negative potentials.

The dose dependence of inhibition was determined by exposing cells to various concentrations of NKA. The resultant data were combined, and a dose-inhibition curve was constructed (Fig. 1C). The averaged, normalized data were fit with a Hill equation, yielding an EC_{50} of 9.8 nM and a Hill coefficient of 0.93. A significant fraction of current (~44%) was apparently not inhibited by the highest concentration of NKA (10 μM). This large residual current probably reflects the fact that NK1 receptors also trigger stimulation of $Ca_V2.3$ that overlaps with inhibition (see below).

As shown in Fig. 1D, the onset of inhibition seemed to contain both fast and slow components (see also Fig. 3, A and B). We did not attempt to quantify these components because application of NKA was relatively slow in our experiments (see *Materials and Methods*). Upon washout of NKA, current amplitudes slowly returned to near control levels and in some cells over-recovered, consistent with the presence of overlapping channel stimulation (see below). The complete recovery of current amplitudes typically required 1 to 2 min of washout.

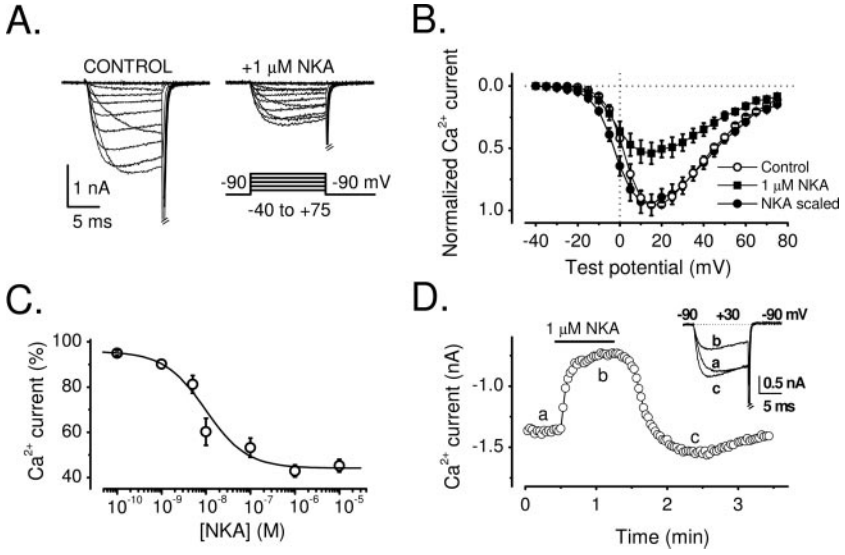

Fig. 1. Strongly activated NK1 receptors inhibit the amplitudes, alter the voltage dependence of activation, and accelerate inactivation of $Ca_V2.3$ currents. A, current families recorded from the same cell before and during exposure to 1 μM NKA. Currents were evoked at 0.2 Hz by depolarizations from −90 to −40 through +75 mV in 5-mV increments. C = 26 pF; R_S = 2.5 MΩ. B, NKA shifts the voltage dependence of activation to slightly more negative potentials over a limited range of test potentials. I-V relationships were determined for six cells before (○) and during (■) inhibition by 1 μM NKA. Voltage protocol is as described in A. I-V relationships were normalized to the maximal control current in each cell, typically recorded at +15 or +20 mV. To facilitate comparison with control currents, the average I-V relationship for inhibited currents (●) was scaled by 1.765 (the ratio of 0.955, which was the maximum normalized average of control currents evoked at +15 mV, to 0.541, the corresponding maximum normalized average current evoked at +15 mV during inhibition by NKA). In these recordings, the average R_S was 2.3 ± 0.2 MΩ, the average maximal current amplitude was 1708 ± 412 pA, and the average maximal voltage-error was 3.8 ± 0.9 mV (n = 6). C, average dose-response relationship for inhibition. Currents were evoked at 0.5 Hz by step depolarizations from −90 to +30 mV. Each cell was exposed to a single concentration of NKA. Symbols represent mean ± S.E.M. of 5 to 30 cells. The smooth curve represents the fit of the average data to the Hill equation: Ca^{2+} current (% of initial) = $(100 - D)/[1 + ([NKA])/EC_{50})^{n_H}]$, where D, the percentage of Ca^{2+} current that could not be inhibited, is 44.1%. The EC_{50} was 9.8 nM, and the Hill coefficient (n_H) was 0.93. D, time course of NKA-mediated inhibition and washout. Currents were evoked at 0.5 Hz by steps from −90 to +30 mV. Current amplitudes are plotted as a function of time. Application of 1 μM NKA is indicated by a thick horizontal line. Inset, Ca^{2+} currents recorded at the indicated times. These currents show that inactivation of $Ca_V2.3$ is significantly accelerated during and after modulation through NK1 receptors. C = 13 pF; R_S = 5.1 MΩ.

Individual Ca^{2+} currents, recorded at the indicated times, are illustrated in Fig. 1D. These currents are shown to introduce an additional aspect of modulation, namely, that exposure to NKA significantly accelerated inactivation of $Ca_V2.3$ currents. This kinetic effect is described in greater detail below (Fig. 5).

Because substance P is an important natural agonist for the NK1 receptor, we also evaluated the effects of this neuropeptide. Inhibition of $Ca_V2.3$ by 1 μM substance P was quantitatively similar (52 ± 2%; n = 3) to that produced by 1 μM NKA. However, the effects of substance P were not readily reversible, and this agonist was thus deemed unsuitable for the present purposes. By contrast, the effects of NKA were reliably reversed upon washout, allowing us to confirm recovery of current amplitudes and to thereby distinguish channel modulation from channel rundown.

Neither NKA nor substance P evoked any modulation of $Ca_V2.3$ in cells that had not been transfected with NK1 receptors, suggesting that HEK293 cells lack endogenous tachykinin receptors. Furthermore, in cells transfected with NK1 receptors and ancillary Ca^{2+} channel α2-δb and β3 subunits, but no $Ca_V2.3$ subunit, whole-cell currents (typically <20 pA) were unaffected by NKA (data not shown). It is therefore unlikely that modulation of endogenous cation channels (e.g., TRP family channels) contributed to our results.

$Ca_V2.3$ Was Primarily Stimulated during Weak Activation of NK1 Receptors. While performing the above-mentioned dose-response experiments, we noticed that very low concentrations of NKA triggered considerable stimulation of $Ca_V2.3$ but little inhibition. This concentration-dependent effect of NKA is documented in Fig. 2A. On average, a low concentration of NKA (1 nM) evoked 39 ± 3% stimulation but only 7 ± 1% inhibition of $Ca_V2.3$ current amplitudes (n = 30 cells). Similar concentration-dependent modulation of $Ca_V2.3$ was seen in experiments where the bath contained a more physiological concentration of Ca^{2+} (Fig. 2C). For example, with 5 mM external Ca^{2+}, 1 nM NKA stimulated current amplitudes by 73 ± 10% and inhibited current amplitudes by 16 ± 3% (n = 12). A high concentration of NKA (1 μM) evoked similar inhibition with either 5 mM Ca^{2+} (65 ± 3%; n = 12) or 40 mM Ca^{2+} (57 ± 3%; n = 30) in the bath. Both the onset and recovery from stimulation (in response to 1 nM NKA) exhibited slow kinetics (Fig. 2, A and C), consistent with our previous reports (Meza et al., 1999; Melliti et al., 2000; Bannister et al., 2004).

Stimulation Was Mediated by PKC. Previous studies have shown that $Ca_V2.3$ is stimulated by muscarinic acetylcholine and metabotropic glutamate receptors acting through PKC (Stea et al., 1995; Meza et al., 1999; Melliti et al., 2000; Kamatchi et al., 2003; Bannister et al., 2004). As shown in Fig. 2E, stimulation of $Ca_V2.3$ through NK1 receptors was blocked by 500 nM Bis I, a specific inhibitor of PKC. In contrast, stimulation was not blocked by 500 nM Bis V, an inactive control compound for Bis I (Fig. 2F). We also tested 1 μM PP2, a Src inhibitor, because NK1 receptors were previously reported to form scaffolding complexes with Src tyrosine kinases (DeFea et al., 2000). PP2 had no effect on stimulation (Fig. 2F). However, staurosporine, which also blocks PKC, eliminated stimulation. These results indicate that PKC mediates stimulation of $Ca_V2.3$ through NK1 receptors.

Because NK1 receptors trigger both stimulation and inhibition of $Ca_V2.3$ currents, the true magnitude of inhibition is probably underestimated in the above-mentioned data summaries. Consistent with this possibility, inhibition evoked by 1 nM NKA was substantially larger (35 ± 4%; n = 9) in cells exposed to 500 nM Bis I than in control cells (7 ± 1%; n = 30).

L-, N-, and P/Q-Type Channels Were Inhibited, but Not Stimulated, by NK1 Receptors. We next asked whether NK1 receptors could modulate Ca^{2+} channel types other than $Ca_V2.3$. To this end, HEK293 cells were transfected with NK1 receptors and either $Ca_V1.3$ (L-type), $Ca_V2.1$ (P/Q-type), or $Ca_V2.2$ (N-type) plus ancillary α2-δ and β subunits. The response of $Ca_V1.3$ to the low concentration (1 nM) of NKA could not be reliably distinguished from rundown, but $Ca_V2.1$ and $Ca_V2.2$ were clearly inhibited, by 24 ± 6% (n = 6) and 43 ± 5% (n = 8), respectively. In each of the above-mentioned experiments,1 nM NKA failed to evoke discernible stimulation of $Ca_V1.3$, $Ca_V2.1$, or $Ca_V2.2$. The high concentration (1 μM) of NKA also failed to evoke stimulation and instead produced 74 ± 5% (n = 6), 61 ± 4% (n = 6), and 79 ± 3% (n = 7) inhibition of these channel types, respectively. We did not attempt to determine whether inhibition of these non–R-type channels was voltage-dependent or -independent, because this issue seems complex (Kammermeier et al., 2000). In summary, our data show that $Ca_V1.3$, $Ca_V2.1$, and $Ca_V2.2$ were inhibited, but not stimulated, through NK1

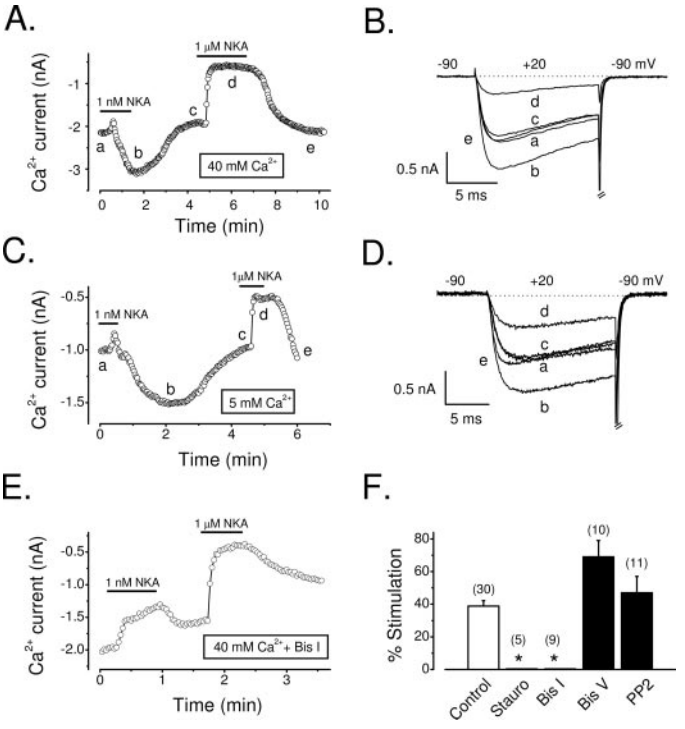

Fig. 2. $Ca_V2.3$ is primarily stimulated during weak activation of NK1 receptors. A, a low concentration (1 nM) of NKA triggers substantial stimulation of $Ca_V2.3$ but very little inhibition. Currents were evoked by 12.5-ms steps to +20 mV delivered at 0.5 Hz. The bath contained 40 mM Ca^{2+}. C = 28 pF; R_S = 2.4 MΩ. B, individual currents recorded at the times indicated in A. C, experiment performed with 5 mM Ca^{2+} in the bath. C = 43 pF; R_S = 2.4 MΩ. D, individual currents recorded at the times indicated in C. E, NKA evokes inhibition but no stimulation of $Ca_V2.3$ currents in the presence of the PKC inhibitor Bis I. F, histograms summarize percentage of stimulation of $Ca_V2.3$ currents in response to 1 nM NKA. Asterisks (*) indicate significant difference (p < 0.05) from controls. Inhibitors were used at 100 nM (staurosporine), 500 nM (Bis I), 500 nM (Bis V), and 1 μM (PP2).

receptors. Inhibition of $Ca_V1.3$ required strongly activated NK1 receptors, whereas even weakly activated NK1 receptors produced significant inhibition of $Ca_V2.1$ and $Ca_V2.2$. In our experiments, $Ca_V2.3$ was the only channel that was stimulated through NK1 receptors.

NK1 Receptors Coupled to PTX- and CTX-Insensitive G Proteins and Inhibited $Ca_V2.3$ Independently of Protein Kinases. NK1 receptors couple primarily to $G\alpha_{q/11}$ in native cells (Macdonald et al., 1996). However, when overexpressed in non-native cells, these receptors may also couple to $G\alpha_s$ and $G\alpha_o$ (Roush and Kwatra, 1998). To test for potential involvement of $G\alpha_s$ and $G\alpha_o$ in modulating $Ca_V2.3$, we pretreated cells with 1 μg/ml PTX for 4 h before electrophysiological experiments. In our hands, this concentration and duration of PTX exposure completely blocks inhibition of N-type ($Ca_V2.2$) calcium channels through $G\alpha_i$-coupled κ-opioid receptors (data not shown). In similar experiments, cells were exposed to freshly prepared CTX (1 μg/ml) for 17 to 22 h before patch-clamp recordings. As summarized in Fig. 3, both PTX and CTX failed to reduce inhibition of $Ca_V2.3$ currents in response to 1 μM NKA. However, inhibition was significantly reduced (to 27 $\pm$ 4%; n = 10) in cells dialyzed for at least 5 min with a pipette solution containing 1 mM GDPβS (Fig. 3C). These data suggest that a toxin-insensitive G protein (presumably $G\alpha_{q/11}$) mediated modulation of $Ca_V2.3$ in our experiments.

As also shown in Fig. 3C, inhibition was not decreased by either 500 nM Bis I or 100 nM staurosporine. In fact, the magnitude of inhibition was significantly larger in cells exposed to these compounds ($p < 0.05$). Staurosporine is a broad-spectrum inhibitor of serine/threonine kinases (including PKC). The larger inhibition in the presence of these kinase inhibitors may partly reflect the fact that PKC-mediated stimulation of $Ca_V2.3$ prevents accurate measurement of inhibition. In addition, PKC-dependent phosphorylation probably interferes with inhibition of $Ca_V2.3$ by G$\beta\gamma$ subunits (Bannister et al., 2004). We also tested 1 μM PP2 and 50 μM genistein, the latter being a broad-spectrum inhibitor of tyrosine kinases. Neither PP2 nor genistein reduced inhibition of $Ca_V2.3$ in response to 1 μM NKA (Fig. 3C). These data suggest that inhibition of $Ca_V2.3$ through NK1 receptors did not involve serine/threonine kinases or tyrosine kinases.

$G\alpha_{q/11}$ and G$\beta\gamma$ Both Mediated Inhibition of $Ca_V2.3$. We next explored the molecular mechanism(s) of inhibition by expressing proteins that sequester either $G\alpha_{q/11}$ or G$\beta\gamma$ subunits. Figure 4A illustrates a representative experiment for a cell transfected with rod transducin ($G\alpha_t$), which effectively buffers G$\beta\gamma$ dimers but is not expected to couple to receptors other than rhodopsin (Kammermeier et al., 2000). In $G\alpha_t$-transfected cells, 1 μM NKA inhibited current amplitudes by only 29 $\pm$ 3% (n = 6), significantly less than in control cells (Fig. 4E). Furthermore, the onset of inhibition seemed qualitatively slower in $G\alpha_t$-expressing cells (Fig. 4A). Similar results were obtained in cells transfected with MAS-GRK3ct, which has also been shown to buffer G$\beta\gamma$ dimers (Kammermeier et al., 2000). The reduced magnitude and slowed onset of inhibition in $G\alpha_t$- and MAS-GRK3ct-expressing cells is consistent with the idea that G$\beta\gamma$ mediates a fast component of inhibition. It would seem that the remaining slow component of inhibition is mediated by $G\alpha_{q/11}$. To examine this possibility, we expressed RGS3T, which previous studies have shown to be a particularly effective antagonist of $G\alpha_{q/11}$-mediated signaling (Scheschonka et al., 2000; Bannister et al., 2002). In RGS3T-expressing cells, application of 1 μM NKA triggered rapid inhibition of current amplitude followed by a relaxation or "sag" to a lower, plateau level of inhibition. This sag corresponds to the onset of PKC-dependent channel stimulation (see below). All together, 1 μM NKA inhibited current amplitudes by 44 $\pm$ 3% (n = 17) in RGS3T-expressing cells, significantly less than inhibition (60 $\pm$ 5%; n = 6) in matched control cells (Fig. 4E). Inhibition was similarly attenuated (41 $\pm$ 3%; n = 14) by expression of PLCβ1ct (Fig. 4E), which also antagonizes $G\alpha_{q/11}$ signaling (Kammermeier et al., 2000). The above-mentioned results suggest that G$\beta\gamma$ mediated a fast component, whereas $G\alpha_{q/11}$ mediated a slow component of inhibition. However, we note that G$\beta\gamma$ might have additionally contributed to the slow component and $G\alpha_{q/11}$ to the fast component of inhibition if these G protein subunits were incompletely buffered in our experiments (see *Discussion*).

As shown in Fig. 4C, inhibition in response to 1 μM NKA was greatly diminished when both $G\alpha_t$ and RGS3T were expressed in the same cell. Under these conditions, 1 μM NKA triggered substantial stimulation (46 $\pm$ 7%; n = 9) but very little inhibition (7 $\pm$ 3%; n = 8) of $Ca_V2.3$ currents. This residual stimulation was completely blocked by Bis I (Fig. 4D) but not by Bis V (data not shown). On average, the high concentration of NKA (1 μM) inhibited current amplitudes by

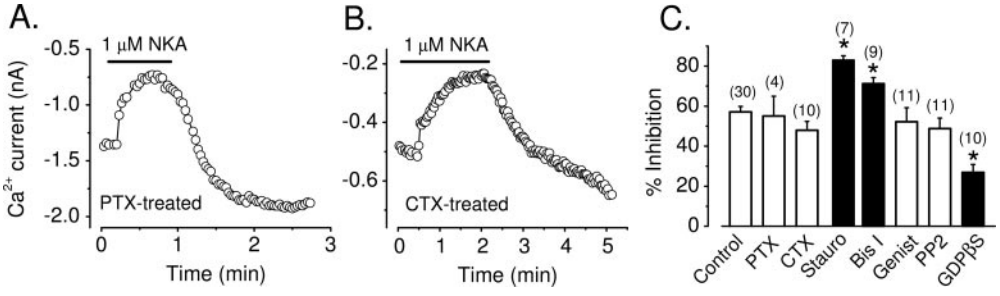

Fig. 3. NK1 receptors couple to PTX- and CTX-insensitive G proteins and inhibit $Ca_V2.3$ independently of protein kinases. A, inhibition of $Ca_V2.3$ in response to 1 μM NKA is insensitive to PTX. Currents were evoked at 0.5 Hz by 10-ms steps from −90 to +30 mV. Current amplitudes are plotted versus time for a cell pretreated with 1 μg/ml PTX. C = 20 pF; R_S = 2.1 MΩ. B, inhibition of $Ca_V2.3$ in response to 1 μM NKA is insensitive to CTX. Currents were evoked at 0.5 Hz by 12.5-ms depolarizations from −90 to +30 mV. Current amplitudes are plotted for a cell pretreated with 1 μg/ml CTX. C = 15 pF; R_S = 2.7 MΩ. C, Histograms summarize percent inhibition of $Ca_V2.3$ currents in response to 1 μM NKA. Inhibitors were used at 100 nM (staurosporine), 500 nM (Bis I), 50 μM (genistein), 1 μM (PP2), and 1 mM (GDPβS). Asterisks (*) indicate significant difference ($p < 0.05$) from controls.

18 ± 4% (n = 9) in cells that expressed both $G\alpha_t$ and RGS3T and exposed to 500 nM Bis I (Fig. 4E). These data clearly show that $G\alpha_{q/11}$ and $G\beta\gamma$ both contribute to inhibition of $Ca_V2.3$ through NK1 receptors. This seems to be the first report that $Ca_V2.3$ is inhibited through a $G\alpha_{q/11}$-dependent signaling mechanism.

The residual modulation of $Ca_V2.3$ observed in cells transfected with both $G\alpha_t$ and RGS3T (Fig. 4, C–E) was somewhat unexpected, because we had previously found that $G\alpha_{q/11}$-mediated stimulation of $Ca_V2.3$ was strongly blocked by expression of either regulator of G protein signaling protein 2 or PLCβ1ct (Melliti et al., 2000). Furthermore, we previously observed that $G\alpha_{q/11}$-mediated inhibition of the L-type channel $Ca_V1.2c$ was virtually eliminated by expression of RGS3T (Bannister et al., 2002). The residual modulation might be explained if $G\alpha_{q/11}$ and $G\beta\gamma$ were incompletely buffered by $G\alpha_t$ and RGS3T in our present experiments. On the other hand, the residual modulation might indicate the involvement of another toxin-insensitive G protein (e.g., $G\alpha_{12/13}$) in addition to $G\alpha_{q/11}$. To explore the latter possibility, we expressed the RGS domain of p115RhoGEF (p115RGS), previously shown to function as a GTPase-activating protein for $G\alpha_{12}$ and $G\alpha_{13}$ (Kozasa et al., 1998). In cells transfected with p115RGS in pcDNA3.1$^-$, application of 1 nM NKA evoked robust stimulation (43 ± 8%; n = 7), whereas 1 μM NKA evoked substantial inhibition (66 ± 5%; n = 8) of $Ca_V2.3$ currents (data not shown). These magnitudes of stimulation and inhibition are indistinguishable from those obtained in control cells. To ensure that we recorded exclusively from cells expressing p115RGS, we fused it to the carboxyl terminus of EGFP. In response to 1 nM NKA, $Ca_V2.3$ currents were stimulated by 42 ± 3% (n = 9) in cells expressing EGFP-p115RGS, compared with 36 ± 15% (n = 5) stimulation in matched controls ($p > 0.05$). In response to the high concentration (1 μM) of NKA, currents were inhibited by 61 ± 3% (n = 6) in EGFP-p115RGS cells and by 67 ± 8% (n = 4) in matched controls ($p > 0.05$). Although these experiments are not exhaustive, they suggest that $G\alpha_{12/13}$ did not play a significant role in modulating $Ca_V2.3$ through NK1 receptors in our system.

NK1 Receptors Accelerated Inactivation of $Ca_V2.3$. As first mentioned in relation to Fig. 1D, the inactivation kinetics of $Ca_V2.3$ currents were noticeably accelerated after exposure to NKA. This effect was quantified by fitting individual Ca^{2+} currents with a single exponential function to obtain time constants for macroscopic activation and inactivation. As shown in Fig. 5B, inactivation of $Ca_V2.3$ currents was clearly accelerated by NKA. For example, currents evoked at +20 mV inactivated with an average time constant ($\tau_{inact.}$) of 33 ± 2 ms (n = 6) before and 18 ± 2 ms (n = 5) after a continuous 2-min exposure to 1 μM NKA ($p < 0.001$). Figure 5D shows that inactivation was significantly accelerated at most test potentials. The acceleration of inactivation was not due to increased bath temperature during NKA application, because temperature was continuously monitored both before and during NKA applications and did not vary by more than ±0.5°C. Furthermore, acceleration was not attributable to decreasing R_S, because membrane charging speed was monitored before and after NKA application and R_S either remained constant or increased during the recordings.

By contrast, the activation kinetics of $Ca_V2.3$ did not seem to be significantly accelerated by NKA (Fig. 5A). Thus, at a test potential of +20 mV, currents activated with an average time constant ($\tau_{act.}$) of 1.5 ± 0.3 ms before and 1.2 ± 0.3 ms (n = 6) after a continuous 2-min exposure to 1 μM NKA; this difference was not significant ($p > 0.05$). Figure 5C plots average values of $\tau_{act.}$ at various test potentials. Activation was significantly accelerated only at a test potential of +10 mV ($\tau_{act.}$ = 1.8 ± 0.3 ms before and 1.2 ± 0.2 ms after NKA exposure; n = 6; p = 0.03; paired t test).

Inhibition of current amplitudes consistently attained stable levels before acceleration of inactivation had became complete. We quantified this relationship by measuring times

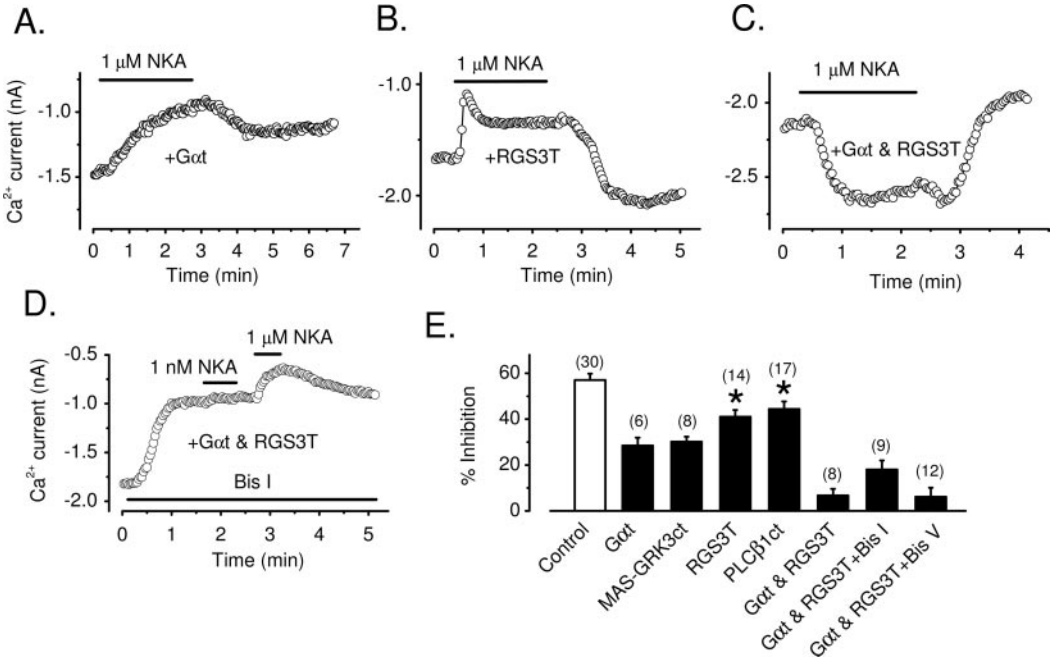

Fig. 4. $G\alpha_{q/11}$ and $G\beta\gamma$ both inhibit $Ca_V2.3$. A, expression of $G\alpha_t$, which buffers $G\beta\gamma$, blocks a fast component of inhibition. Currents were evoked at 0.5 Hz by 12.5-ms depolarizations to +25 mV. C = 17 pF; R_S = 2.5 MΩ. B, expression of RGS3T, which buffers $G\alpha_{q/11}$, blocks a slow component of inhibition. Currents were evoked at 0.5 Hz by 12.5-ms depolarizations to +30 mV. C = 14 pF; R_S = 4.9 MΩ. C, coexpression of Gαt and RGS3T in the same cell greatly reduces inhibition but not stimulation. Currents were evoked at 0.5 Hz by 12.5-ms depolarizations to +20 mV. C = 30 pF; R_S = 3.0 MΩ. D, stimulation is blocked by Bis I (500 nM) in cells coexpressing both $G\alpha_t$ and RGS3T. C = 29 pF; R_S = 4.1 MΩ. E, histograms summarize percentage of inhibition in response to 1 μM NKA. Asterisks (*) indicate significant difference ($p < 0.05$) from controls.

required for inhibition and acceleration to near completion. Measuring from the beginning of NKA application, inhibition of current amplitude was 90% complete in 15 ± 1 s, whereas acceleration of inactivation required 28 ± 3 s (n = 5) to attain 90% completion. As illustrated in Fig. 5E, current amplitudes also recovered more quickly than inactivation rate after NKA washout. This difference in recovery was consistently observed (four of five cells). We did not extensively pursue the mechanism underlying acceleration of inactivation. However, it may be worth mentioning that inactivation was significantly accelerated in cells exposed to 100 nM Bis I [$\tau_{inact.}$ at 20 mV was 36 ± 1 ms before and 23 ± 1 ms (n = 7) after a continuous 1- to 2-min application of 1 μM NKA], suggesting that PKC is not involved.

Discussion

This work shows that NK1 receptors triggered complex modulation of $Ca_V2.3$ (R-type) Ca^{2+} channels. We have identified three distinct signaling mechanisms involved in this modulation: a fast inhibition mediated by Gβγ, a slow inhibition mediated by $G\alpha_{q/11}$, and a slow stimulation mediated by PKC (Fig. 6). We note that the stimulatory effect predominated during low receptor occupancy, whereas the three forms of modulation produced overlapping influences on $Ca_V2.3$ during high receptor occupancy. We also find that NK1 receptors markedly accelerated inactivation of $Ca_V2.3$. The increased rate of inactivation further reduced R-type Ca^{2+} influx during modulation through NK1 receptors.

We present evidence that $G\alpha_{q/11}$ as well as Gβγ mediated inhibition of $Ca_V2.3$ through NK1 receptors (Fig. 4). This finding is in general agreement with Kammermeier et al. (2000), who showed that $G\alpha_{q/11}$ and Gβγ are both required for voltage-independent inhibition of native N-type Ca^{2+} channels by NK1 receptors heterologously expressed in rat sympathetic neurons. In the present experiments, we found that separately buffering Gβγ or $G\alpha_{q/11}$ partially blocked inhibition of $Ca_V2.3$ and altered the time course of inhibition (Fig. 4). We also found that simultaneously buffering both Gβγ and $G\alpha_{q/11}$ in the same cells greatly reduced inhibition (Fig. 4C) but did not eliminate it (Fig. 4, D and E). It is intriguing that substantial stimulation of $Ca_V2.3$ current was observed in cells where Gβγ and $G\alpha_{q/11}$ were simultaneously buffered (Fig. 4C). Although we did not rigorously quantify the time course of channel modulation in our experiments, our results are consistent with the notion that Gβγ mediated a fast component of inhibition, whereas $G\alpha_{q/11}$ mediated a slow component (Fig. 6). However, our data do not exclude the possibility that Gβγ also contributed to slow inhibition or that $G\alpha_{q/11}$ contributed to fast inhibition.

Previous studies indicate that $G\alpha_{q/11}$ mediates slow inhibition of L-type ($Ca_V1.2c$) and N-type ($Ca_V2.2$) Ca^{2+} channels (Melliti et al., 2001; Bannister et al., 2002). Our present finding that $G\alpha_{q/11}$ triggered slow inhibition of $Ca_V2.3$ suggests that this form of inhibition is conserved among different classes of Ca^{2+} channels. We did not attempt to identify the molecular mechanism of slow inhibition here, beyond showing that $G\alpha_{q/11}$ was involved, because this would have

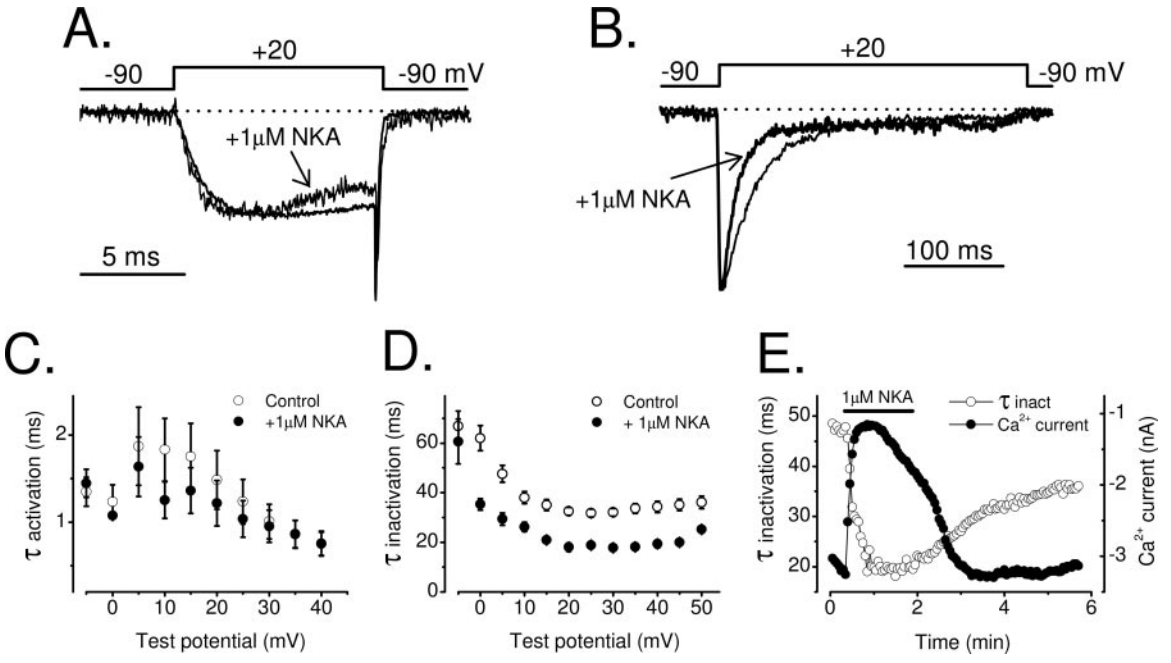

Fig. 5. NK1 receptors significantly accelerate the inactivation kinetics of $Ca_V2.3$. A, activation. Currents were recorded from the same cell before (light trace) and 130 s after (bold trace) continuous exposure to 1 μM NKA. The inhibited current is scaled for comparison. C = 28 pF; R_S = 2.4 MΩ. B, inactivation. Currents were recorded from the same cell before (light trace) and 100 s after (bold trace) application of 1 μM NKA. The inhibited current is scaled for comparison. C = 29 pF; R_S = 3.8 MΩ. C, on average, activation of $Ca_V2.3$ is not significantly accelerated by NKA. Average time constants of activation (τ activation) are plotted as a function of test potential. Symbols represent mean ± S.E.M. of four to six cells. Data from currents evoked at 0.5 Hz by 10-ms depolarizations from −90 to −5 through +40 mV in 5-mV increments. Current families were evoked before application of NKA (○) and during maximal inhibition by 1 μM NKA (●). D, inactivation is significantly accelerated at all test potentials except −5 mV. Average time constants of inactivation (τ inactivation) are plotted as a function of test potential. Symbols represent mean ± S.E.M. of five to six cells. Currents evoked at 0.5 Hz by 300-ms depolarizations from −90 to −5 through +50 mV in 5-mV increments. Current families were evoked before application of NKA (○) and during maximal inhibition by 1 μM NKA (●). E, comparison of the time courses for inhibition of current amplitudes and acceleration of inactivation. C = 53 pF; R_S = 2.9 MΩ. Currents were evoked at 0.33 Hz by 300-ms steps from −90 to +20 mV.

required extensive additional experiments (Gamper et al., 2004). However, depletion of membrane phosphoinositol-4,5-bisphosphate (PIP_2) is a strong candidate for this mechanism (Fig. 6), because PIP_2 depletion seemed to underlie slow $G\alpha_{q/11}$-mediated inhibition of both N-type (see Gamper et al., 2004) and P/Q-type calcium channels (Wu et al., 2002). It is also theoretically possible that $G\alpha_{q/11}$ inhibited $Ca_V2.3$ directly (Fig. 6).

We found that NK1 receptors shifted the voltage dependence of $Ca_V2.3$ activation to slightly more negative potentials (Fig. 1B). This finding agrees with a recent demonstration by Tai et al. (2006) that the voltage dependence of activation of native R-type currents is shifted to negative potentials during modulation by muscarinic acetylcholine receptors. It is worth noting that the negative shift in voltage dependence reported here and by Tai et al. (2006) is *opposite* that typically observed for G protein-inhibited channels of the Ca_V2 family. Additional experiments are needed to elucidate the underlying mechanism. However, because application of exogenous PIP_2 shifts the voltage dependence of activation of $Ca_V2.1$ (Wu et al., 2002) and $Ca_V2.2$ (Gamper et al., 2004) to more *positive* potentials, we hypothesize that depletion of endogenous PIP_2 might underlie the negative shift in $Ca_V2.3$ activation (Fig. 6).

We find that $Ca_V2.3$ was preferentially stimulated during weak activation of NK1 receptors (Fig. 2). By contrast, $Ca_V2.3$ was both inhibited and stimulated during strong activation of NK1 receptors. This remarkable "bipolar" modulation of $Ca_V2.3$ might have important physiological consequences if NK1 receptors experience widely varying concentrations of agonist in vivo, as seems probable.

Preferential triggering of stimulation by weakly activated NK1 receptors probably reflects the presence of considerable biochemical amplification within the stimulatory pathway (Fig. 6). This pathway likely involved sequential activation of three enzymes: $G\alpha_{q/11}$, PLCβ, and PKC. By contrast, G$\beta\gamma$-mediated inhibition probably reflected direct binding of G$\beta\gamma$ to $Ca_V2.3$ with little or no amplification. Depletion of membrane PIP_2 would most simply involve sequential activation of only two enzymes, $G\alpha_{q/11}$ and PLCβ. These differences in biochemical amplification might help to explain our results with G$\beta\gamma$- and $G\alpha_{q/11}$-buffering proteins. We found that buffering both G$\beta\gamma$ and $G\alpha_{q/11}$ in the same cells (by coexpressing $G\alpha_t$ and RGS3T) blocked inhibition of $Ca_V2.3$ more effectively than it blocked stimulation (Fig. 4, C–E). In principle, it should be easier to block G$\beta\gamma$- and $G\alpha_{q/11}$-mediated inhibition of $Ca_V2.3$ than $G\alpha_{q/11}$-mediated stimulation because of the greater theoretical amplification involved in stimulation. The apparent ineffectiveness of RGS3T in blocking stimulation of $Ca_V2.3$ (Fig. 4C) may be explained if only a few $G\alpha_{q/11}$ needed to escape buffering by RGS3T to activate PKC.

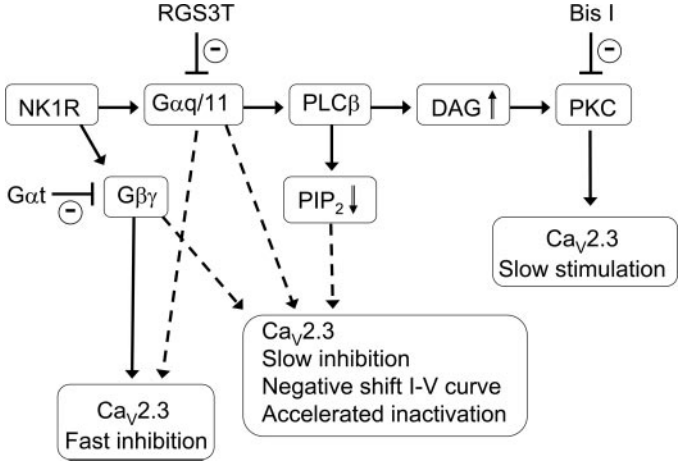

Fig. 6. Schematic summary of results. Solid arrows indicate well established signaling pathways and mechanisms of channel modulation. Dashed arrows indicate less well established signaling pathways that might modulate $Ca_V2.3$. For example, if G$\beta\gamma$ was incompletely buffered by $G\alpha_t$ or MAS-GRK3ct in our experiments, it might contribute to slow inhibition of $Ca_V2.3$. Likewise, if $G\alpha_{q/11}$ was incompletely buffered by RGS3T or PLCβ1ct, it might contribute to fast inhibition of $Ca_V2.3$. Depletion of PIP_2 has not been experimentally demonstrated to modulate $Ca_V2.3$. Finally, the diagram postulates that $G\alpha_{q/11}$ might modulate $Ca_V2.3$ through direct interaction.

Stimulation of R-type currents has been demonstrated in native cells. For example, Yu and Shinnick-Gallagher (1998) showed that native R-type currents are stimulated through corticotropin-releasing factor receptors in central amygdala neurons. In addition, Tai et al. (2006) showed that native R-type currents are stimulated through muscarinic acetylcholine and metabotropic glutamate receptors in hippocampal CA1 neurons. Our present experiments indicate that PKC mediated stimulation of $Ca_V2.3$ through NK1 receptors (Fig. 2), consistent with previous observations that $Ca_V2.3$ is stimulated by phorbol esters or $G\alpha_{q/11}$-coupled muscarinic acetylcholine receptors or metabotropic glutamate receptors (Stea et al., 1995; Meza et al., 1999; Melliti et al., 2000; Kamatchi et al., 2003; Bannister et al., 2004). Tai et al. (2006) found that native hippocampal R-type currents are stimulated through a Ca^{2+}-independent, diacylglycerol-dependent PKC isoform, in agreement with our previous study of cloned $Ca_V2.3$ channels (Bannister et al., 2004).

The ability of NK1 receptors to both inhibit and stimulate $Ca_V2.3$ suggests that native R-type currents might be modulated in a dynamic fashion during activation of $G\alpha_{q/11}$-coupled receptors. As one possibility, G$\beta\gamma$-mediated inhibition of $Ca_V2.3$ could be selectively blocked by recruiting G$\beta\gamma$-binding proteins (e.g., G protein-coupled receptor kinases) to receptor-channel complexes. Likewise, $G\alpha_{q/11}$-mediated inhibition of $Ca_V2.3$ could be selectively blocked by recruiting RGS proteins or downstream effectors of $G\alpha_{q/11}$ besides PLCβ. As suggested by our results (Fig. 4C), antagonizing both G$\beta\gamma$ and $G\alpha_{q/11}$ signaling at the same time could substantially reduce inhibition of $Ca_V2.3$, but leave stimulation relatively intact. Selective blockade of inhibition could thereby have significant consequences for physiological processes involving R-type Ca^{2+} influx.

Our present results may be relevant to understanding molecular mechanisms of nociception and other neurobiological processes. NK1 receptors are involved in diverse physiological functions, including nociception, aggression, anxiety, asthma, cough, depression, emesis, irritable bowel syndrome, and migraine (De Felipe et al., 1998; Duffy, 2004). Likewise, $Ca_V2.3$ has been shown to participate in a variety of processes, including nociception (Saegusa et al., 2000), neurosecretion (Wu et al., 1998; Gasparini et al., 2001), synaptic plasticity (Sabatini and Svoboda, 2000; Breustedt et al., 2003; Dietrich et al., 2003; Yasuda et al., 2003), electrical excitability of central neurons (Kuzmiski et al., 2005; Metz et al., 2005; Tai et al., 2006), cerebellar

function (Osanai et al., 2006), morphine analgesia and tolerance (Yokoyama et al., 2004), and anxiety (Saegusa et al., 2000; Lee et al., 2002). NK1 receptors are expressed at high densities in the dorsal horn of the spinal cord and in the amygdala, hippocampus, and striatum (Duffy, 2004). $Ca_V2.3$ is similarly expressed in spinal cord dorsal horn (Saegusa et al., 2000), amygdala (Lee et al., 2002), and hippocampus and striatum (Niidome et al., 1992). Thus, these two proteins are expressed together in common regions of the nervous system and are implicated in some of the same neurological functions. It therefore seems plausible that NK1 receptors could modulate $Ca_V2.3$ within nociceptive pathways and other neurological circuits.

R-type currents are important in determining the electrical properties of hippocampal neurons. For example, R-type currents contribute to afterdepolarizations and bursting activity of hippocampal CA1 neurons (Metz et al., 2005), and receptor-mediated stimulation of R-type currents profoundly alters the dendritic integration and intrinsic resonance properties of these neurons by shifting the pattern of Ca^{2+} influx from L-, N-, and P/Q-type channels to R-type channels (Tai et al., 2006). R-type currents are also critical in shaping Ca^{2+} dynamics in dendritic spines of hippocampal CA1 neurons (Sabatini and Svoboda, 2000; Yasuda et al., 2003). In spines, native R-type currents can be inhibited through G protein-coupled receptors (Sabatini and Svoboda, 2000) or brief trains of action potentials (Yasuda et al., 2003); intriguingly, the latter form of inhibition blocks θ-burst-induced long-term potentiation (Yasuda et al., 2003). We speculate that stimulation, as well as inhibition, of R-type currents influences synaptic plasticity at dendritic spines. It also seems plausible that receptor-mediated stimulation of R-type currents contributes to plateau potentials and spiking in dorsal horn and other neurons.

The present study provides new information concerning R-type channels and NK1 receptors. This information may help in understanding the molecular basis of nociception, electrical excitabililty, synaptic plasticity and other physiological processes.

Acknowledgments

We thank Dr. Keith Elmslie (Penn State College of Medicine, Hershey, PA) and Dr. Katarina Stroffekova (Utah State University, Logan, UT) for helpful suggestions regarding organization and content of the manuscript. Dr. Karim Melliti made the original observation that $Ca_V2.3$ is inhibited through a slow Gαq/11-mediated pathway.

References

Bannister RA, Melliti K, and Adams BA (2002) Reconstituted slow muscarinic inhibition of neuronal ($Ca_V1.2c$) L-type Ca^{2+} channels. *Biophys J* **83:**3256–3267.

Bannister RA, Melliti K, and Adams BA (2004) Differential modulation of $Ca_V2.3$ Ca^{2+} channels by Gq/11-coupled muscarinic receptors. *Mol Pharmacol* **65:**381–388.

Breustedt J, Vogt KE, Miller RJ, Nicoll RA, and Schmitz D (2003) α1E-containing Ca^{2+} channels are involved in synaptic plasticity. *Proc Natl Acad Sci USA* **100:**12450–12455.

DeFea KA, Vaughn ZD, O'Bryan EM, Nishijima D, Dery O, and Bunnett NW (2000) The proliferative and antiapoptotic effects of substance P are facilitated by formation of a β-arrestin-dependent scaffolding complex. *Proc Natl Acad Sci USA* **97:**11086–11091.

De Felipe C, Herrero JF, O'Brien JA, Palmer JA, Doyle CA, Smith AJ, Laird JM, Belmonte C, Cervero F, and Hunt SP (1998) Altered nociception, analgesia and aggression in mice lacking the receptor for substance P. *Nature (Lond)* **392:**394–397.

Dietrich D, Kirschstein T, Kukley M, Pereverez A, von der Brelie C, Schneider T, and Beck H (2003) Functional specialization of presynaptic $Ca_V2.3$ Ca^{2+} channels. *Neuron* **39:**483–496.

Duffy RA (2004) Potential therapeutic targets for neurokinin-1 receptor antagonists. *Expert Opin Emerg Drugs* **9:**9–21.

Gamper N, Reznikov V, Yamada Y, Yang J, and Shapiro MS (2004) Phosphatidylinositol 4,5-bisphosphate signals underlie receptor-specific Gq/11-mediated modulation of N-type Ca^{2+} channels. *J Neurosci* **24:**10980–10992.

Gasparini S, Kasyanov AM, Pietrobon D, Voronin LL, and Cherubini E (2001) Presynaptic R-type calcium channels contribute to fast excitatory synaptic transmission in the rat hippocampus. *J Neurosci* **21:**8715–8721.

Humeau Y, Herry C, Kemp N, Shaban H, Fourcaudot E, Bissiere S, and Luthi A (2005) Dendritic spine heterogeneity determines afferent-specific Hebbian plasticity in the amygdala. *Neuron* **45:**119–131.

Kamatchi GL, Tiwari SN, Chan CK, Chen D, Do SH, Durieux ME, and Lynch C III (2003) Distinct regulation of expressed calcium channels 2.3 in *Xenopus* oocytes by direct or indirect activation of protein kinase C. *Brain Res* **968:**227–237.

Kammermeier PJ, Ruiz-Velasco V, and Ikeda SR (2000) A voltage-independent calcium current inhibitory pathway activated by muscarinic agonists in rat sympathetic neurons requires both $G\alpha_{q/11}$ and $G_\beta\gamma$. *J Neurosci* **20:**5623–5629.

Kohlmeier KA and Leonard CS (2006) Transmitter modulation of spike-evoked calcium transients in arousal related neurons: muscarinic inhibition of SNX-482-sensitive calcium influx. *Eur J Neurosci* **23:**1151–1162.

Kozasa T, Jiang X, Hart MJ, Sternweis PM, Singer WD, Gilman AG, Bollag G, and Sternweis PC (1998) p115 RhoGEF, a GTPase activating protein for Gα12 and Gα13. *Science (Wash DC)* **280:**2109–2111.

Kubota M, Murakoshi T, Saegusa H, Kazuno A, Zong S, Hu Q, Noda T, and Tanabe T (2001) Intact LTP and fear memory but impaired spatial memory in mice lacking $Ca_V2.3$ (α1E) channel. *Biochem Biophys Res Commun* **282:**242–248.

Kuzmiski JB, Barr W, Zamponi GW, and MacVicar BA (2005) Topiramate inhibits the initiation of plateau potentials in CA1 neurons by depressing R-type calcium channels. *Epilepsia* **46:**481–489.

Lee SC, Choi S, Lee T, Kim HL, Chin H, and Shin HS (2002) Molecular basis of R-type calcium channels in central amygdala neurons of the mouse. *Proc Natl Acad Sci USA* **99:**3276–3281.

Macdonald SG, Dumas JJ, and Boyd ND (1996) Chemical cross-linking of the substance P (NK-1) receptor to the α subunits of the G proteins G_q and G_{11}. *Biochemistry* **35:**2909–2916.

Melliti K, Meza U, and Adams B (2000) Muscarinic stimulation of α1E Ca channels is selectively blocked by the effector antagonist function of RGS2 and phospholipase C-beta1. *J Neurosci* **20:**7167–7173.

Melliti K, Meza U, and Adams B (2001) RGS2 blocks slow muscarinic inhibition of N-type Ca^{2+} channels reconstituted in a human cell line. *J Physiol (Lond)* **532:**337–347.

Metz AE, Jarsky T, Martina M, and Spruston N (2005) R-type calcium channels contribute to afterdepolarization and bursting in hippocampal CA1 pyramidal neurons. *J Neurosci* **25:**5763–5773.

Meza U, Bannister R, Melliti K, and Adams B (1999) Biphasic, opposing modulation of cloned neuronal α1E Ca channels by distinct signaling pathways coupled to M2 muscarinic acetylcholine receptors. *J Neurosci* **19:**6806–6817.

Murakami M, Nakagawasai O, Suzuki T, Mobarakeh II, Sakurada Y, Murata A, Yamadera F, Miyoshi I, Yanai K, Tan-No K, et al. (2004) Antinociceptive effect of different types of calcium channel inhibitors and the distribution of various calcium channel alpha 1 subunits in the dorsal horn of spinal cord in mice. *Brain Res* **1024:**122–129.

Newcomb R, Szoke B, Palma A, Wang G, Chen X, Hopkins W, Cong R, Miller J, Urge L, Tarczy-Hornoch K, et al. (1998) Selective peptide antagonist of the class E calcium channel from the venom of the tarantula *Hysterocrates gigas*. *Biochemistry* **37:**15353–15362.

Niidome T, Kim MS, Friedrich T, and Mori Y (1992) Molecular cloning and characterization of a novel calcium channel from rabbit brain. *FEBS Lett* **308:**7–13.

Osanai M, Saegusa H, Kazuno AA, Nagayama S, Hu Q, Zong S, Murakoshi T, and Tanabe T (2006) Altered cerebellar function in mice lacking $Ca_V2.3$ Ca^{2+} channel. *Biochem Biophys Res Commun* **344:**920–925.

Piedras-Rentería ES and Tsien RW (1998) Antisense oligonucleotides against α1E reduce R-type calcium currents in cerebellar granule cells. *Proc Natl Acad Sci USA* **95:**7760–7765.

Roush ED and Kwatra MM (1998) Human substance P receptor expressed in Chinese hamster ovary cells directly activates $G\alpha_{q/11}$, $G\alpha_S$, and $G\alpha_O$. *FEBS Lett* **428:**291–294.

Sabatini BL and Svoboda K (2000) Analysis of calcium channels in single spines using optical fluctuation analysis. *Nature (Lond)* **408:**589–593.

Saegusa H, Kurihara T, Zong S, Minowa O, Kazuno A, Han W, Matsuda Y, Yamanaka H, Osanai M, Noda T, et al. (2000) Altered pain responses in mice lacking α1E subunit of the voltage-dependent Ca^{2+} channel. *Proc Natl Acad Sci USA* **97:**6132–6137.

Scheschonka A, Dessauer CW, Sinnarajah S, Chidiac P, Shi CS, and Kehrl JH (2000) RGS3 is a GTPase-activating protein for $G_i\alpha$ and $G_q\alpha$ and a potent inhibitor of signaling by GTPase-deficient forms of $G_q\alpha$ and $G_{11}\alpha$. *Mol Pharmacol* **58:**719–728.

Sochivko D, Pereverzev A, Smyth N, Gissel C, Schneider T, and Beck H (2002) The $Ca_V2.3$ Ca^{2+} channel subunit contributes to R-type Ca^{2+} currents in murine hippocampal and neocortical neurons. *J Physiol (Lond)* **542:**699–710.

Stea A, Soong TW, and Snutch TP (1995) Determinants of PKC-dependent modulation of a family of neuronal calcium channels. *Neuron* **15:**929–940.

Tai C, Kuzmiski JB, and MacVicar BA (2006) Muscarinic enhancement of R-type calcium currents in hippocampal CA1 pyramidal neurons. *J Neurosci* **26:**6249–6258.

Tottene A, Volsen S, and Pietrobon D (2000) α1E subunits form the pore of three cerebellar R-type calcium channels with different pharmacological and permeation properties. *J Neurosci* **20:**171–178.

Wu L, Bauer CS, Zhen XG, Xie C, and Yang J (2002) Dual regulation of voltage-gated calcium channels by PtdIns(4,5)P2. *Nature (Lond)* **419:**947–952.

Wu LG, Borst JG, and Sakmann B (1998) R-type Ca^{2+} currents evoke transmitter release at a rat central synapse. *Proc Natl Acad Sci USA* **95:**4720–4725.
Yasuda R, Sabatini BL, and Svoboda K (2003) Plasticity of calcium channels in dendritic spines. *Nat Neurosci* **6:**948–955.
Yokoyama K, Kurihara T, Saegusa H, Zong S, Makita K, and Tanabe T (2004) Blocking the R-type ($Ca_V2.3$) Ca^{2+} channel enhanced morphine analgesia and reduced morphine tolerance. *Eur J Neurosci* **20:**3516–3519.
Yu B and Shinnick-Gallagher P (1998) Corticotropin-releasing factor increases dihydropyridine- and neurotoxin-resistant calcium currents in neurons of the central amygdala. *J Pharmacol Exp Ther* **284:**170–179.
Zhang JF, Randall AD, Ellinor PT, Horne WA, Sather WA, Tanabe T, Schwarz TL, and Tsien RW (1993) Distinctive pharmacology and kinetics of cloned neuronal Ca^{2+} channels and their possible counterparts in mammalian CNS neurons. *Neuropharmacology* **32:**1075–1088.

Address correspondence to: Dr. Brett Adams, Department of Biology, Utah State University, 5305 Old Main Hill, Logan, UT 84322. E-mail: brett@biology.usu.edu